

Novel method for wavelength locking of tunable diode lasers based on photoacoustic spectroscopy

Dávid Tátrai¹, Zoltán Bozóki^{1,2} and Gábor Szabó¹

1. University of Szeged, Department of Optics and Quantum Electronics
6720, Hungary, Szeged, Dóm tér 9.
2. MTA-SZTE Research Group on Photoacoustic Spectroscopy
6720, Hungary, Szeged, Dóm tér 9.

Phone: +3662543744

Fax.: +3662544658

E-mail address: tatraid@titan.physx.u-szeged.hu

Abstract

A novel wavelength locking method for tunable diode lasers based on a photoacoustic (PA) detection unit is presented. A wavelength modulated laser is repeatedly tuned over an absorption line of a small molecule in the gaseous phase and the generated PA signal is recorded. In the phase variation curve of the recorded PA signal there is a *180 degree* phase reversal around the peak of the absorption line and the corresponding inflection point is a characteristic wavelength feature to be used for wavelength locking. An automated algorithm has been developed which has less than two seconds execution time if the optical absorption coefficient at the peak of the absorption line is at least $2 \times 10^{-5} \text{ cm}^{-1}$. With this algorithm the wavelength of a near-infrared distributed feedback (DFB) diode laser can be locked with an absolute accuracy of *60 fm* (i.e. relative accuracy of 4×10^{-8}) or better even at atmospheric sample gas pressure. As there is no need to stabilize the gas pressure or temperature or the concentration of the light absorbing component and the PA detection unit can be easily integrated into various experimental set-ups, the proposed method has the potential to be applicable even under demanding industrial or field conditions.

Keywords

DFB diode laser, wavelength locking, photoacoustic spectroscopy

1. Introduction

In various applications of single mode tunable diode lasers it is crucially important to lock the laser wavelength with high accuracy. A typical example is optical absorption spectroscopy based gas concentration measurements, e.g. with distributed feedback (DFB) single mode diode lasers in the near-infrared region. In this application the wavelength stability and accuracy of the laser is especially critical whenever the measurement is performed either at varying total gas pressures or on a multi-component gas sample which contains components with overlapping optical absorption spectra at the wavelength(s) of the measurement [1-2]. Another important example is the telecommunication industry [3-4].

The wavelength of DFB diode lasers can vary directly due to variations in the environmental conditions, especially of the ambient temperature [5]. Furthermore the variations of the environmental temperature due to the non-zero temperature coefficients of electronic components and their ageing can cause drifts of the set laser temperature and set operational current causing a wavelength variation. Moreover the wavelength can vary spontaneously due to the so called ageing effects [6-7]. Due to the non-controllable ageing effects the stabilization of all the environmental parameters which effect the wavelength of the laser is insufficient and the use of an active wavelength locking mechanism is required.

DFB diode lasers can be tuned by changing either the temperature or the applied driving current. Temperature tuning can be performed with the help of a Peltier element and an NTC (negative temperature coefficient) thermistor integrated into the laser package [8]. With temperature tuning the wavelength of the diode laser can be tuned with response time typically in the seconds range, and with tuning efficiency of $\approx 0.1 \text{ nm/K}$. The laser driving current can also be

used for wavelength tuning with a typical efficiency of $\approx 5 \text{ pm/mA}$ and with a response time in the sub-millisecond range. The numerical values of these tuning efficiencies vary from laser to laser but they are characteristic to a given one.

The possibility of laser wavelength locking with relative accuracy of $\lambda/\Delta\lambda=10^{-14}$ has already been demonstrated [9] which even makes possible to measure the fortuitous drift of fundamental physical constants like Plank constant or electron charge [10]. The goal of the work presented here is not to concur with the best available accuracy, but rather to propose a simple, robust, widely usable and for many applications sufficiently accurate method operable even under non-laboratory conditions.

This paper is organized as follows. A brief overview of the available wavelength locking techniques is followed by the description of the applied photoacoustic (PA) detection unit and its supplementary experimental setup. Next the suggested wavelength locking method is presented followed by the results of the test measurements. In the appendix a theoretical description of the proposed method is given.

2. Overview of the currently available wavelength locking methods

Wavelength locking is usually performed by comparing the wavelength of a light source to a reference wavelength followed by the elimination of the measured difference. By illuminating through a wavelength etalon with the laser beam and recording the output light intensity spectrum, a characteristic spectral feature which e.g. belongs to a local extreme value for the transmitted light power can be searched and the laser wavelength can be locked to this wavelength feature. All the commonly used wavelength etalons, e.g. high finesse Fabry-Perot

interferometers, high resolution monochromators, narrow bandwidth Lyot-filters [11] have certain disadvantages. In general it is rather challenging to build them into a sufficiently robust construction applicable outside optical laboratories and they are usually rather expensive especially whenever highly accurate wavelength locking is required. Very often the uncertainty of the wavelength locking is increased considerably by the wavelength instability of the etalon itself.

Using the absorption or emission spectra of atoms or small molecules in the gaseous phase for wavelength locking purposes is a straightforward approach as these absorption lines are fairly narrow and under stable environmental conditions (i.e. constant pressure, temperature and gas composition) their spectral characteristics do not vary. As an example with Lamb dip spectroscopy based wavelength locking on low pressure gases having Doppler broadened absorption lines relative accuracy of $\lambda/\Delta\lambda=10^{10}$ can be achieved [12]. However it is rather difficult to apply this method either on pressure broadened absorption lines or under non-ideal measurement conditions e.g. outside of an optical laboratory.

Recently an alternative wavelength locking method which is based on photoacoustic (PA) signal generation and detection has been suggested [13]. In the proposed method the wavelength of a wavelength modulated laser is tuned over an absorption line of water vapor and a characteristic feature in the recorded PA signal is used as wavelength reference. The relative accuracy with which the wavelength of the laser can be locked was found to be about $\Delta\lambda/\lambda=3\times 10^{-7}$ while the method also has the advantage of short execution time especially compared to step by step recording the absorption spectra. However the method has certain disadvantages too: the wavelength of the selected absorption feature was found to be rather sensitive to the

environmental conditions especially to the gas pressure, and in some cases the wavelength determination with the method is equivocal. That is why a similar but improved method is presented here which is also based on simultaneous wavelength modulation and tuning over a molecular absorption line combined with PA signal generation and detection, but instead of the amplitude rather the phase of the generated PA signal is used for wavelength locking purposes as it will be described below.

3. The photoacoustic effect

The PA effect, discovered by A.G. Bell [11-12], is the conversion from light to acoustic energy through the consecutive processes of light absorption, non-radiative molecular relaxation, local heating, thermal expansion and sound wave generation. If a gas sample is illuminated by a train of light pulses, or by intensity or wavelength modulated light, which are at least partially absorbed by the sample, the absorbed light energy generates acoustic waves. In most of the PA experimental arrangements the measured gas sample is introduced into an acoustic resonator, which amplifies the acoustic signal which in turn is measured by a sensitive microphone. The microphone signal is usually processed by using either lock-in or synchronized sampling technique. Nowadays tunable lasers or optical parametric oscillators are commercially available from the near UV to the mid IR. This huge variety of light sources and the development of sensitive and stable microphones has given the possibility of developing sensitive and selective gas analysis systems based on PA spectroscopy [13].

Rosencwaig and Gersho [14] have shown that the amplitude of the acoustic wave generated by the PA effect is proportional to the modulated part of the absorbed light power. In

case of neglecting an instrument specific phase shift, from the theory of Fourier transformation it follows that the PA signal is proportional to the time derivate of the absorbed laser power:

$$PA \propto \frac{d}{dt} P_{abs}, \quad (1)$$

where P_{abs} is the absorbed light power and t is time. In case of weak absorption the amplitude of the microphone signal is a linear function of the absorbance. Indeed linearity over several orders of magnitude of concentration was observed in various PA measurements [15].

4. Experimental

4.1. The PA detection unit for wavelength locking

The PA detection unit consists of a DFB diode laser, a longitudinal differential PA detection cell [19] supplemented with a pressure transducer and a computer controlled DSP (digital signal processing) based electronic unit, which controls the diode laser and amplifies and processes the microphone signal. Furthermore it performs signal generation and evaluation for the wavelength locking method as it is described below. This unit has been already successfully used in various gas detection applications [16].

The PA detection cell is filled with atmospheric air and the wavelength locking is performed on one of the absorption lines of water vapor. The diode laser (NEL NLK1E5E1AA) used in the reported demonstration measurements is tunable in the 1392 ± 1 nm wavelength range. The tuning efficiencies of the diode laser have been determined by tuning it through this wavelength range, recording the PA spectrum of water vapor absorption lines and comparing this spectrum with that is listed in the PNNL spectroscopic database [20]. Based on this comparison

the temperature and current tuning efficiencies of the laser are 101 pm/K , and 4.9 pm/mA , respectively. The temperature of the laser chip has been actively stabilized by the electronics with an estimated accuracy of 1 mK or better, i.e. the wavelength instability of the laser due to temperature instability is equal or less than 100 fm . The laser current can be set by the electronics with a resolution of about $4 \text{ }\mu\text{A}$, i.e. the laser wavelength can be set by the driving current with a resolution of about 15 fm . For wavelength locking the absorption line of water vapor corresponding to the $J'K'_{1}K''_{1}=660 \leftarrow J''K''_{1}K'_{1}=661$ transition within the $\nu_1 + \nu_3$ combination band has been used. The peak optical absorption coefficient and the half width of the absorption line at atmospheric pressure are $3.3 \times 10^{-4} \text{ cm}^{-1}$ (@ 1% water vapor concentration) and 25 pm , respectively.

4.2. The wavelength locking method

Simultaneous wavelength modulation and tuning over the absorption line can be generated by repeatedly feeding the diode laser with the following driving current waveform:

$$I(t) = I_0 + gt + h \sin(2\pi ft) \quad 0 \leq t \leq T_{ep}, \quad (2)$$

where I_0 is the time independent part of the current, g is the slope of the current ramp, h is the amplitude of the current modulation, f is the frequency of the modulation and T_{ep} is the temporal length of an excitation period. The temporal variation of the absorbed light power by the sample gas generates the PA signal in accordance with Equation 1. The signal to noise ratio of the wavelength locking procedure has been increased by repeating the excitation sequence and averaging together the generated microphone signal sequences by using synchronized sampling

technique. Parameters of the wavelength locking procedure applied in the reported measurements are listed in Table 1.

The generated microphone signal $S(t)$ is processed by performing a numerical Gabor-transformation [21] on it at the laser modulation frequency as follows:

$$G\{S(t)\} = \frac{1}{\sqrt{2\pi}} \int_{t-\frac{T}{2}}^{t+\frac{T}{2}} S(t') e^{i2\pi ft'} dt', \quad (3)$$

where T is the temporal length of one laser modulation period ($T=1/f$). The phase variation curve is calculated as:

$$\varphi(t) = \arctan \frac{\text{Im}[G\{S(t)\}]}{\text{Re}[G\{S(t)\}]} - \frac{2\pi}{T} \text{mod } 2\pi \quad (4)$$

where Im and Re denotes the imaginary and real parts, respectively and the second term on the right hand side accounts for the phase of the laser modulation. Finally, the laser driving current which corresponds to the inflection point of the phase variation curve (which is called in the following as *locking current* and the corresponding wavelength as *locking wavelength*) is determined numerically by searching for the maximum value of the derivative of the phase variation curve.

4.3. Supplementary set-up

In order to study the effect of the temperature and pressure of the sample gas on the performance of the wavelength locking algorithm the PA detection unit was supplemented with the following components. First of all a heating unit was applied with which the temperature of

the PA detection cell and consequently also the temperature of the measured gas sample could be stabilized to any value between 290 and 330 K with an accuracy of ± 0.1 K. Furthermore a gas handling unit was added with which the pressure of the sample gas could be varied between 100 and 1000 mbar. As it can be seen on Figure 1 the gas handling unit contains a humidifier for generating variable water vapor concentration in the measured gas, a stepper motor controlled needle valve for setting the gas pressure in the PA cell, a mass flow controller ensuring a stable gas flow rate through the cell and a vacuum pump for sucking the humidified air through the PA cell.

4.4. Characterization and testing

Dependence of the accuracy of the wavelength locking method on temperature: the wavelength locking procedure was repeatedly performed at PA detection cell temperatures of 295 , 305 , 315 , and 325 K. During this test the gas pressure was stabilized at 950 ± 1 mbar.

Dependence of the accuracy of the wavelength locking method on pressure: as the primary planned application of the proposed wavelength locking method is atmospheric water vapor measurement with a photoacoustic instrument operated on-board of a research or passenger aircraft [22], pressure dependence was studied in the pressure range typical for this application, i.e. at pressures between 100 and 1000 mbar. During this test the PA cell temperature was stabilized at 325 ± 0.1 K.

Long term accuracy test: The wavelength locking procedure was continuously repeated for 30 days, while the temperature and the pressure of the gas was stabilized to 325 ± 0.1 K and to 950 ± 1 mbar, respectively. Furthermore every day once the PA spectrum of the water vapor absorption line was also recorded by setting the ramp parameter (g in Equation 2) to zero and by

changing the un-modulated part of the diode laser driving current (I_0 in Equation 2) step-by-step. On the recorded spectrum a centered Voigt profile was fitted. In comparison with the proposed wavelength locking procedure this measurement has the disadvantage of being rather time consuming and the fitting algorithm requires rather large computational capacity. On the other hand one of the fitting parameters, i.e. the current value which corresponds to the center of the absorption line varies in perfect correlation with the variation in the locking current therefore it can be used as a reference.

Dependence of the accuracy of the wavelength locking method on the optical absorption coefficient: In this test the wavelength locking algorithm was repeatedly executed while with the help of the humidifier the water vapor concentration was gradually increased from 10 to 10000 ppmV corresponding to the variation of the peak optical absorption coefficient in the range of $3.3 \times 10^{-7} - 3.3 \times 10^{-4} \text{ cm}^{-1}$. Each microphone signal sequence generated by the excitation sequence of Equation 2 was recorded for post-processing. During post-processing subsequent microphone signal sequences were averaged together before performing the Gabor transformation based wavelength locking algorithm as described above. In the following the symbol N denotes the number of microphone signal sequences averaged together and the accuracy of wavelength locking as a function of N at various peak optical absorption coefficients was investigated. During this test the temperature and the pressure of the gas were stabilized to $40 \pm 0.1 \text{ }^\circ\text{C}$ and $950 \pm 1 \text{ mbar}$, respectively.

5. Results and discussion

An example of the measured microphone signals and the calculated phase variation curves can be seen on Figure 2. a-b.

During the temperature test the numerical value of the locking current was found to be independent from the PA cell (and correspondingly to the gas) temperature. This proves that in the studied temperature range neither the temperature induced line broadening nor the central wavelength shift of the absorption line has measurable effect on the wavelength locking procedure. Consequently the temperature stabilization of the PA detection cell is actually not required for the proposed wavelength locking method.

Contrary to the temperature, the gas pressure was found to influence the locking wavelength as it can be seen on Figure 3, where the y-axis was calculated by multiplying the relative variation of the locking current with the current tuning rate of the diode laser. The measured pressure dependence can be accurately approximated with a parabola:

$$\Delta\lambda = \lambda_0 + 5.405 \times p - 0.00188 \times p^2 \quad (5)$$

where $\Delta\lambda$ is the variation of the locking wavelength in *fm*, λ_0 is the extrapolated locking wavelength at *0 mbar*, p is the pressure in *mbar*. It should be noted that this pressure dependence coincides quite well to the results of Hejje et al [23] who measured the pressure dependent line shift of the same absorption line. This pressure dependence necessitates the continuous measurement of the gas pressure and the application of a correction on the locking wavelength in accordance with Equation 5. With a commercially available general purpose pressure sensor the gas pressure can be measured with an accuracy and precision of *1 mbar*, which according to Equation 5 corresponds to a locking wavelength inaccuracy of less than *4 fm* throughout the

entire measured pressure range.

During the long term stability test, due to the aging effect of the diode laser, a linear drift in the locking current with a slope of $3.36 \mu A/day$ was observed which can be converted to $16.46 fm/day$ by multiplying it with the measured current tuning coefficient of the laser (Figure 4). The same variation was also observed in the laser current value corresponding to the center of the absorption line marked by closed circles in Figure 4. When this linear drift was subtracted from the measured locking currents, the resulting data had a normal distribution with a standard deviation of $10.6 \mu A$ i.e. $52 fm$. This uncertainty can be considered as an upper limit on the accuracy of the proposed wavelength locking method.

The results of the measurements performed for determining the accuracy of the wavelength locking method on the optical absorption coefficient was evaluated in a way that for each optical absorption coefficient an averaging number (N) was searched above which the wavelength locking accuracy is equal to or better than the $52 fm$ determined during the long term accuracy test. As it can be seen on Figure 5 the measurement time (which is equal to $N \times T_{ep}$) varies with the square root of the optical absorption coefficient. However for optical absorption coefficients which are less than $1.9 \times 10^{-5} cm^{-1}$ the $52 fm$ limit cannot be reached with any N . This limit corresponds to a microphone signal to noise ratio about 30.

6. Conclusion

A novel wavelength locking method, based on the simultaneous laser tuning and modulation over a pressure broadened absorption line, PA signal generation and detection, and a

numerical Gabor transformation based signal processing has been introduced. Results of measurements proved that for a water vapor absorption line in the near infrared the proposed method has an absolute accuracy of at least 52 fm (which corresponds to a relative accuracy of $\lambda/\Delta\lambda = 4 \times 10^{-8}$). This accuracy is at the limit of the wavelength setting capability of the electronics due to its finite current resolution. Besides water vapor, the absorption lines of other small gaseous molecules can be used for wavelength locking with the proposed method as well. The selected reference feature in the phase of the PA signal is univocal and therefore it can be used as a fully automatic wavelength locking method. Besides the short execution time and the accuracy, the main advantage of the method is that it does not require the use of a precise and expensive optical set-up. As the method is insensitive to the gas temperature and has well controllable pressure dependence due to the collisional shifting of the absorption line, there is no need to stabilize the temperature of the PA cell while the gas pressure in the cell can vary as well provided that it is measured and the pressure dependence of the locking wavelength is properly corrected.

Due to the high sensitivity of the PA cell, the proposed method can be executed even on gas samples with low optical absorption coefficient (in the range of 10^{-4} cm^{-1}) at the locking wavelength. In such cases the laser beam in the PA cell suffers almost no attenuation (the length of the PA cell is about 10 cm) and thus the beam leaving the cell is ready for further use. In other words the proposed method does not require the use of e.g. a beam splitter or any moving optical elements, i.e. the wavelength locking unit can be easily integrated into various optical set-ups. As the mechanical stability in case of a PA system is not a critical issue, the method can be applied

even in a rough industrial environment without increasing considerably the complexity of the system into which it is integrated.

Acknowledgements

The research leading to these results has received funding from the European Community's 7th Framework Programme (FP7/2008-2012) under EUFAR contract n° 227159. The project has been partially funded by ‘TAMOP-4.2.1/B- 09/1/KONV-2010-0005—Creating the Center of Excellence at the University of Szeged’ supported by the European Union and co-financed by the European Social Fund. The project has been also partially supported by the OTKA Foundation from the Hungarian Research and Technology Innovation Fund (project numbers K 101905.)

Appendix: Theoretical background

In the following a calculation method is presented with which the observed variation in the phase signal is verified theoretically.

Above the threshold current of diode lasers the wavelength and power of the laser as the function of temperature and current can be given as:

$$\lambda(I, T) = \lambda_0 + aT + bI, \quad (\text{A1})$$

$$P_{laser}(I) = P_0 + fI, \quad (\text{A2})$$

where λ_0 is a virtual wavelength for 0 K temperature and 0 mA current, a is the temperature tuning coefficient, T is the temperature in K, b is the current tuning coefficient, and I is the applied laser diode current, P_0 is the negative virtual power at 0 mA current and f is the slope of the power-current curve above the threshold limit.

The simultaneous wavelength modulation and tuning can be produced with the previously discussed current waveform (2, Fig 6. a.).

The absorption line is described as a Lorentzian profile which is a good approximation for pressure broadened single absorption lines under atmospheric circumstances:

$$\alpha(\lambda) = \alpha_{\max} \frac{\delta^2}{(\lambda - \lambda_{\text{peak}})^2 + \delta^2} \quad (\text{A3})$$

where α_{\max} is the maximum value of the absorption, δ is the FWHM of the absorption line, and λ_{peak} is the wavelength of α_{\max} .

The absorbed power in case of weak absorption can be approximated as:

$$P_{\text{abs}}(t) = P_{\text{laser}}(t)\alpha(t) \quad (\text{A4})$$

As described previously the PA signal is proportional to the time derivate of the absorbed light power (1). Using the above described model (1, 8-10) the photoacoustic signal can be calculated analytically (Fig 6. b) and subsequently the Gabor transform and the phase variation curve (Fig 6. c) can be evaluated numerically. There is a good qualitative agreement between the measured and the calculated phase variation curves. In order to achieve quantitative agreement the applied model has to be extended by taking into account the linewidth of the laser, the modulation broadening properties of the laser, the acoustic properties of the PA cell while a more realistic

mathematical model for the absorption line like Voigt, Rautain or Galatri ones has to be used as well [24].

References:

1. Y. Shimose, T. Okamoto, A. Maruyama, M. Aizawa, H. Nagai, "Remote sensing of methane gas by differential absorption measurement using a wavelength tunable DFB LD," *Photonics Technology Letters* 3, 86 (1991)
2. Y. Sakai, S. Sudo, T. Ikegami, "Frequency stabilization of laser diodes using 1.51-1.55 μm absorption lines of $^{12}\text{C}_2\text{H}_2$ and $^{13}\text{C}_2\text{H}_2$ molecules," *Quantum Electronics* 28, 75 (1992)
3. Y. Park, S. T. Lee, C. J. Chae, "A novel wavelength stabilization scheme using a fiber grating for WDM transmission" *Photonics Technology Letters* 10, 1446 (1998)
4. L. Colace, G. Masini, G. Assanto, "Wavelength stabilizer for telecommunication lasers: design and optimization," *Journal of Lightwave Technology*, 21,0 1749 (2003)
5. H. Ghafouri-Shiraz, "Distributed Feedback Laser Diodes and Optical Tunable Filters," (Wiley 2003)
6. R. Matthey, C. Affolderbach, G. Miletì, "Methods and evaluation of frequency aging in distributed-feedback laser diodes for rubidium atomic clocks," *Optics Letters* 36, 3311 (2011)
7. S. L. Woodward, P. Parayanthal, U. Koren, "The effects of aging on the Bragg section of a DBR laser," *Photonics Technology Letters* 5, 750 (1993)
8. J. Seufert, M. Fischer, J. Koeth, R. Werner, M. Kamp, A. Forchel, "DFB laser diodes in the wavelength range from 760 nm to 2.5 μm ," *Spectrochimica Acta Part A: Molecular and Biomolecular Spectroscopy* 60, 3243 (2004)

9. Th. Udem, R. Holzwarth, T.W. Hänsch, "Optical frequency metrology," *Nature* 416, 233 (2002)
10. M.Fischer, N. Kolachevsky, M. Zimmermann, R. Holzwarth, Th. Udem, T. W. Hänsch, M. Abgrall, J. Grünert, I. Maksimovic, S. Bize, H. Marion, F. Pereira Dos Santos, P. Lemonde, G. Santarelli, P. Laurent, A. Clairon, C. Salomon, M. Haas, U. D. Jentschura, C. H. Keitel, "New limits on the drift of fundamental constants from laboratory measurements" *Physical Review Letters* 92, 230802 (2004)
11. W. Demtröder, "Laser Spectroscopy," (Springer, 2002)
12. W. E. Lamb, Jr., "Theory of an Optical Maser" *Physical Review* 134, A1429 (1964)
13. M. Szakáll, J. Csikós, Z. Bozóki, G. Szabó, "On the temperature dependent characteristics of a photoacoustic water vapor detector for airborne application," *Infrared Physics & Technology* 51, 113 (2007)
14. A.G. Bell, "On the production and reproduction of sound by light: the photophone," *American Journal of Science* 20, 305 (1880)
15. A. G. Bell, "Upon the production of sound by radiant energy," *Philosophical Magazine and Journal of Science* 11, 510 (1881)
16. Z. Bozóki, A. Pogány, G. Szabó, "Photoacoustic instruments for practical applications: present, potentials, and future challenges," *Applied Spectroscopy Reviews* 46, 1 (2011)
17. Rosencwaig, A. Gersho, "Theory of Photoacoustic Effect with Solids," *Journal of Applied Physics* 47, 64 (1976)

18. Z.Bozóki, M. Szakáll, Á. Mohácsi, G. Szabó, Zs. Bor, “Diode laser based photoacoustic humidity sensors,” *Sensors and Actuators B* 91, 219 (2003)
19. A. Miklós, P. Hess, Z. Bozóki, „Application of acoustic resonators in photoacoustic trace gas analysis and metrology,” *Review of Scientific Instruments* 72 1937 (2001)
20. S. W. Sharpe, T. J. Johnson, R. L. Sams, P. M. Chu, G. C. Rhoderick, P. A. Johnson, “Gas-Phase Databases for Quantitative Infrared Spectroscopy,” *Applied Spectroscopy* 58, 1452 (2004)
21. I.N. Bronshtein, K.A. Semendyayev, G. Musiol, H. Mühlig, “Taschenbuch der Mathematik,” (Springer 1999)
22. C. A. M. Brenninkmeijer, P. Crutzen, F. Boumard, T. Dauer, B. Dix, R. Ebinghaus, D. Filippi, H. Fischer, H. Franke, U. Frieß, J. Heintzenberg, F. Helleis, M. Hermann, H. H. Kock, C. Koepfel, J. Lelieveld, M. Leuenberger, B. G. Martinsson, S. Miemczyk, H. P. Moret, H. N. Nguyen, P. Nyfeler, D. Oram, D. O'Sullivan, S. Penkett, U. Platt, M. Püpeck, M. Ramonet, B. Randa, M. Reichelt, T. S. Rhee, J. Rohwer, K. Rosenfeld, D. Scharffe, H. Schlager, U. Schumann, F. Slemr, D. Sprung, P. Stock, R. Thaler, F. Valentino, P. Van Velthoven, A. Waibel, A. Wandel, K. Waschitschek, A. Wiedensohler, I. Xueref-Remy, A. Zahn, U. Zech, H. Ziereis, “Civil Aircraft for the regular investigation of the atmosphere based on an instrumented container: The new CARIBIC system,” *Atmospheric Chemistry and Physics* 7, 18 (2007) 4976
23. Hejie Li, A. Farooq, J. B. Jeffries, R. K. Hanson, “Diode laser measurements of temperature-dependent collisional-narrowing and broadening parameters of Ar-

perturbed H₂O transitions at 1391.7 and 1397.8nm,” *Journal of Quantitative Spectroscopy & Radiative Transfer* 109, 132 (2008)

24. J. Buldyreva, N. Lavrentieva, V. Starikov,” Collisional Line Broadening And Shifting Of Atmospheric Gases; A Practical Guide for Line Shape Modelling by Current Semi-classical Approaches” (Imperial College Press, 2010)

Biographies:

Biographies and photographs of the authors are not available.

Table and caption

Table 1:

Amplitude of current modulation (h)	6 mA
Modulation frequency (f)	7000 Hz
Slope of the current ramp (g)	215 mA/sec
Duration of one excitation and one sampling period (T_{ep})	9 msec
PA signal sampling rate	56000 Hz

Table 1 caption: : Modulation and sampling parameters of the reported wavelength locking procedure

Figure captions:

Figure 1. Schematics of the experimental setup. The PA detection unit (encircled with a dashed line) is supplemented with a temperature stabilization unit, a gas handling system and a humidifier which are used for varying the sample gas temperature, pressure and water vapor concentration, respectively. Thick, thin and wavy lines are representing the gas tubes, the electrical connections and the modulated light beam, respectively

Figure 2. An example of the measured PA signals (a), and the calculated phase variation curves (b).

Figure 3. Dependence of the locking wavelength on the gas pressure within the PA detection cell.

Figure 4. Long term variation of the locking current (left side Y axis) and that of the relative wavelength (right side Y axis). The grey curve is the locking current determined by the proposed algorithm, while closed circles are the current values corresponding to the center of the absorption line determined by Voigt profile fitting. The black line is the result of line fitting to the locking current variation.

Figure 5. The measurement (averaging) time needed for the accuracy of the wavelength locking method to reach the 52 fm limit. Symbols represent measurement results; line is the fitted square root dependence.

Figure 6. The simultaneous wavelength tuning and modulation (a); the calculated PA signal (b), and the phase variation curve (c) with the inflection point.

Figures:

Figure 1:

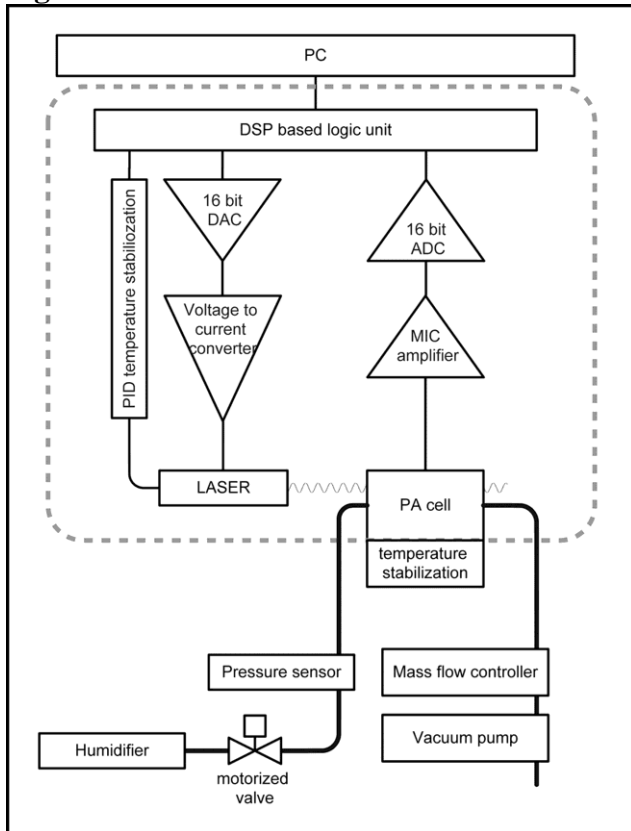


Figure 2:

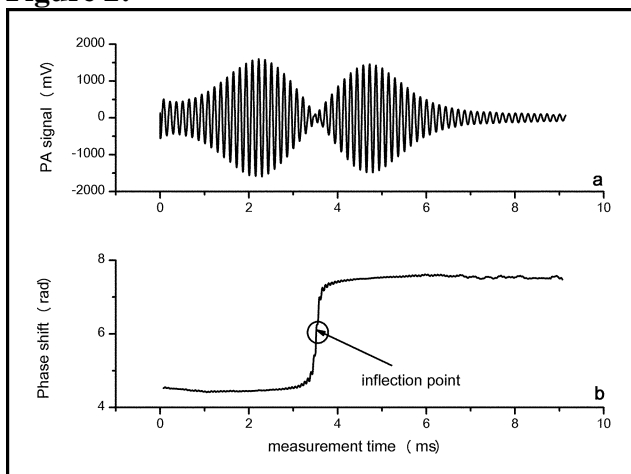


Figure 3:

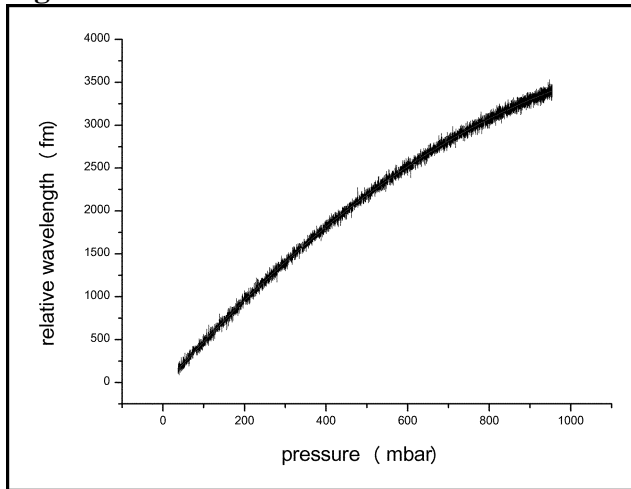


Figure 4:

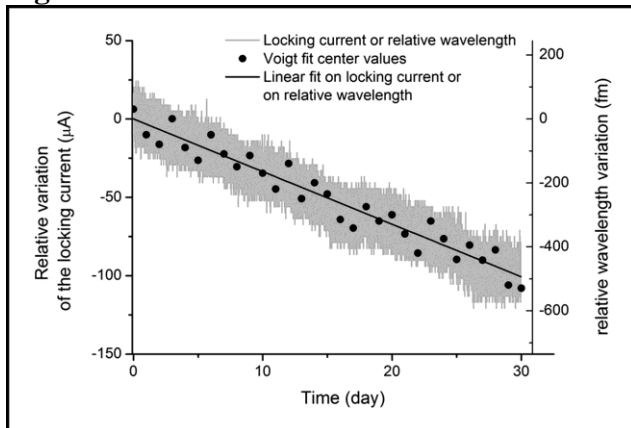


Figure 5:

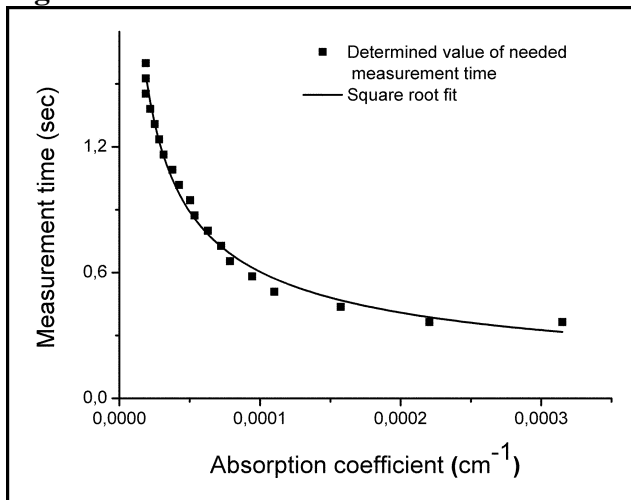


Figure 6:

